Electronic Supplementary Material (ESI) for Journal of Materials Chemistry C.

Electronic supplementary information

High-performance semitransparent organic solar cells based on sequentially processed heterojunction†

Peiyao Xue,[a] Jingming Xin,[c] Guanyu Lu,[d] Boyu Jia,[a] Heng Lu,[a] Guanghao Lu,[d] Wei Ma,[c] Ray P. S. Han,[e] and Xiaowei Zhan[a,b,*]

[a]School of Materials Science and Engineering, Peking University, Beijing 100871, China. *E-mail address*: xwzhan@pku.edu.cn

[b]Key Laboratory of Eco-functional Polymer Materials of Ministry of Education

College of Chemistry and Chemical Engineering

Northwest Normal University, Lanzhou 730070, China

[c]State Key Laboratory for Mechanical Behavior of Materials, Xi'an Jiaotong University, Xi'an 710049, China

[d]Frontier Institute of Science and Technology, Xi'an Jiaotong University, Xi'an 710049, China

[e]Jiangzhong Cancer Research Center, Jiangxi University of Chinese Medicine, Nanchang 330004, China

Materials

PM6 was purchased from Solarmer Materials Inc., Y6 and PNDIT-F3N were purchased from EflexPV Inc., PEDOT:PSS (CLEVIOS^{TM} PVP AI 4083) was purchased from Heraeus Inc. Unless stated otherwise, all chemical reagents and solvents were used without further purification.

Device fabrication

The opaque devices are based on the conventional sandwich structure, indium tin oxide (ITO) glass/PEDOT:PSS/active layer/PNDIT-F3N/Ag. First, the patterned ITO glass (sheet resistance = 15 $\Omega\ \square^{-1}$) was precleaned in the ultrasonic bath with de-ionized water, acetone and isopropanol, respectively. The pre-cleaned ITO glass was treated by ultraviolet-ozone chamber (UVO) (Jelight Company, USA) for 15 min. Then, the PEDOT:PSS layer (*ca.* 30 nm) was spin-coated at 3000 rpm onto the ITO glass, followed by baking at 150 ℃ for 15 min. For BHJ device, PM6:Y6 solution (15 mg mL^{-1} dissolved in chloroform) was spin-coated at 3000 rpm onto the PEDOT:PSS layer to form the photoactive layer. The ratio of donor and acceptor is 1:1 or 1:2. For SHJ device, PM6 solution (6 mg mL^{-1} in chloroform) was spin-coated at 3000 rpm onto the PEDOT:PSS layer to form the bottom layer. Y6 solution (9 mg mL^{-1} in chloroform) was spin-coated at 3000 rpm onto the bottom layer to form the top layer. The thickness of active layer is *ca.* 100 nm, measured by profilometer (Dektak XT). After that, the PNDIT-F3N solution (0.5 mg mL^{-1} in methanol) was spin-coated onto the active layer at 2000 rpm. Finally, Ag electrode layer (*ca.* 80 nm) was then evaporated onto the PNDIT-F3N layer under vacuum (*ca.* 10^{-5} Pa). The measured area of the device was 4

mm^2 (2 mm × 2 mm). The semitransparent devices are based on the following sandwich structure, indium tin oxide (ITO) glass/PEDOT:PSS/active layer/PNDIT-F3N/Au/Ag. The thickness of Au layer is *ca.* 1 nm, and the thickness of Ag layer varies from 10 nm to 17 nm.

Device characterization

The current density-voltage (*J*-*V*) curves were measured using a computer-controlled B2912A Precision Source/Measure Unit (Agilent Technologies). An XES-70S1 (SAN-EI Electric Co., Ltd) solar simulator (AAA grade, 70 × 70 mm^2 photobeam size) coupled with AM 1.5G solar spectrum filters was used as the light source, and the optical power at the sample was 100 mW cm^{-2}. A 2 × 2 cm^2 monocrystalline silicon reference cell (SRC-1000-TC-QZ) was purchased from VLSI Standards Inc. The external quantum efficiency (EQE) spectra were measured using a Solar Cell Spectral Response Measurement System QE-R3011 (Enlitech Co., Ltd.). The light intensity at each wavelength was calibrated using a standard single crystal Si photovoltaic cell.

Characterization

The UV-vis absorption spectra were measured on UV3600Plus spectrophotometer on thin films (on a quartz substrate). Atomic force microscopy (AFM) characterization was performed using a Multimode 8 scanning probe microscope (Bruker Daltonics) in the non-contacting mode. Transmission electron microscopy (TEM) characterization was performed using JEM-2100 operated at 200 keV. Grazing incidence wide-angle X-ray scattering (GIWAXS) measurements were performed at beamline 7.3.3 at the Advanced Light Source (ALS).[S1] The 10 keV X-ray beam was incident at a grazing angle of 0.11°~0.15°. The scattered X-rays were detected using a Dectris Pilatus 2M photon counting detector (Switzerland). The GIWAXS samples were prepared on silicon substrate by spin-coating.

Hole-only and electron-only devices were fabricated using the architectures of ITO glass/PEDOT:PSS/active layer/Au for holes and ITO glass/ZnO/active layer/Ag for electrons. For hole-only devices, the pre-cleaned ITO glass was treated by UVO chamber for 15 min. Then PEDOT:PSS (*ca.* 30 nm) was spin-coated on it, and baked at 150 °C in the drying oven for 15 min. The photoactive layer was spin-coated at 3000 rpm on PEDOT:PSS layer, and Au (*ca.* 80 nm) was evaporated onto the photoactive layer under vacuum. For electron-only devices, ZnO (*ca.* 30 nm) was spin-coated onto the ITO glass, then the photoactive layer was spin-coated at 3000 rpm onto the ZnO layer. At the end, Ag electrode layer (*ca.* 80 nm) was evaporated under vacuum. The mobility was extracted by fitting the *J-V* curves using SCLC method.[S2] The *J-V* curves of the devices were plotted as $\ln(Jd^3/V^2)$ versus $(V/d)^{0.5}$. The equation is as follows:

$$\ln\left(\frac{Jd^3}{V^2}\right) \cong 0.89(1/E_0)^{0.5}(V/d)^{0.5} + \ln(9\varepsilon_0\varepsilon_r\mu/8) \qquad \text{(S1)}$$

where J refers to the current density, μ is hole or electron mobility, ε_r is relative dielectric constant (*ca.* 3), ε_0 is dielectric constant of free space (8.82×10^{-12} F m^{-1}), $V = V_{appl} - V_{bi}$, where V_{appl} is the applied voltage to the device, and V_{bi} is the built-in voltage due to the difference in work function of the electrodes (for hole-only diodes, V_{bi} is 0.2 V; for electron-only diodes, V_{bi} is 0 V). E_0 is characteristic field, and d is the thickness of the active layer.

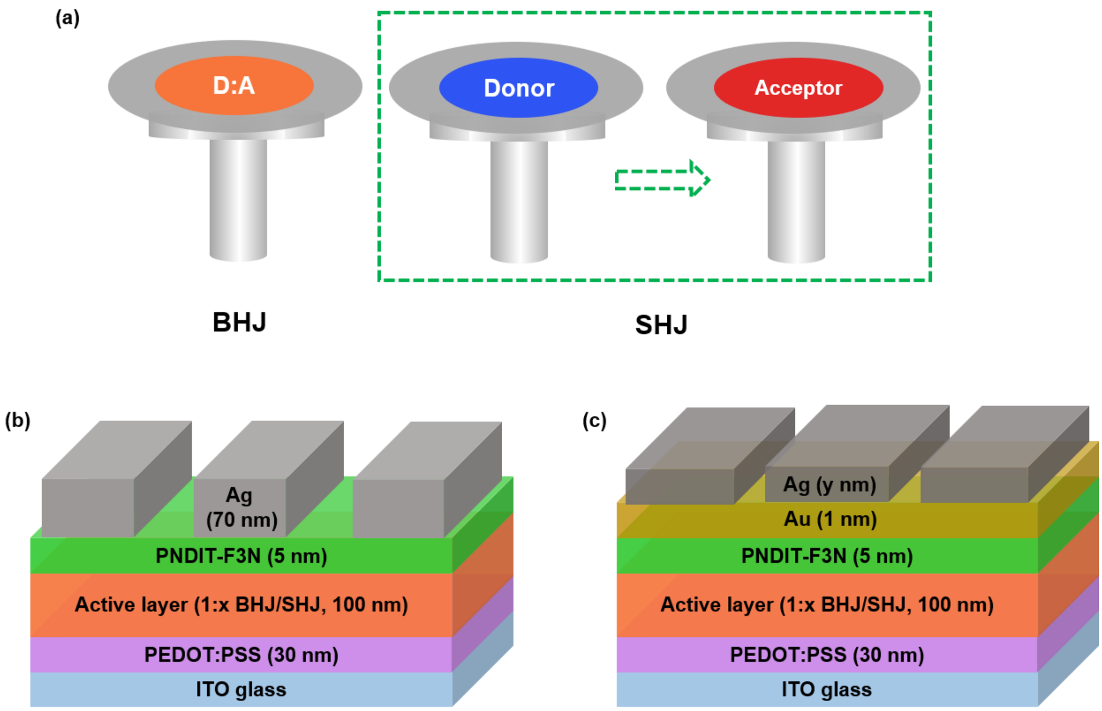

Fig. S1 (a) BHJ and SHJ device fabrication process. The device structure illustration of (b) opaque and (c) semitransparent devices.

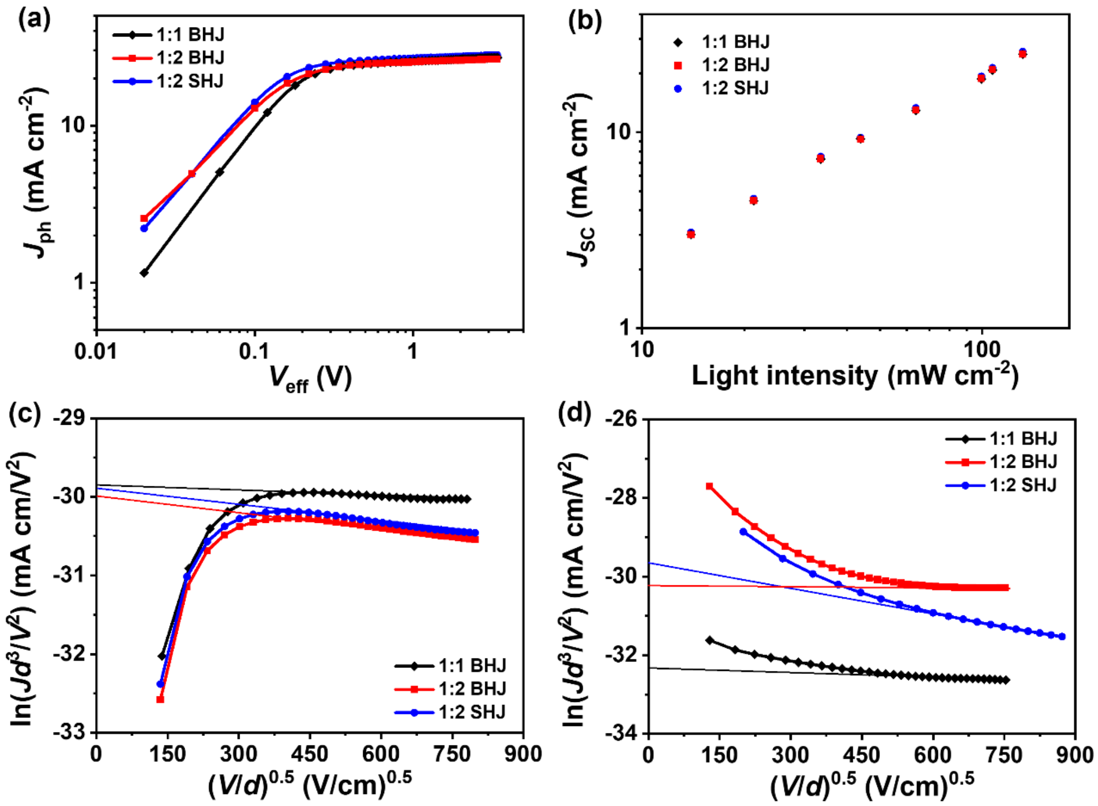

Fig. S2 (a) J_{ph}-V_{eff} curves and (b) J_{SC}-P_{light} curves of 1:1 BHJ, 1:2 BHJ and 1:2 SHJ devices. *J*-*V* characteristics in the dark for hole-only (c) and electron-only (d) devices based on 1:1 BHJ, 1:2 BHJ and 1:2 SHJ blend films.

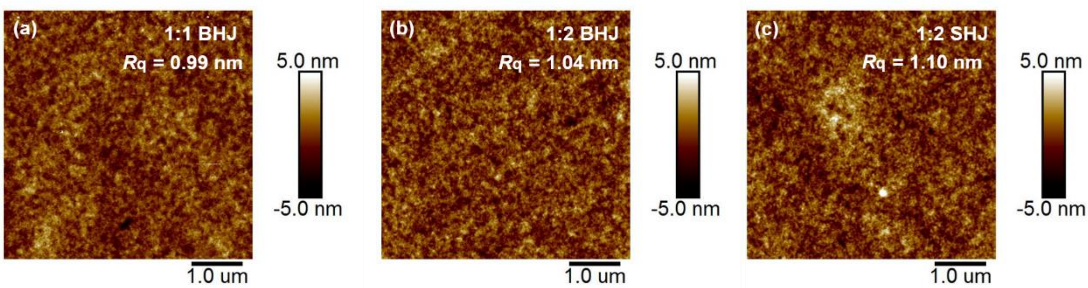

Fig. S3 AFM height images of (a) 1:1 BHJ; (b) 1:2 BHJ and (c) 1:2 SHJ blend films.

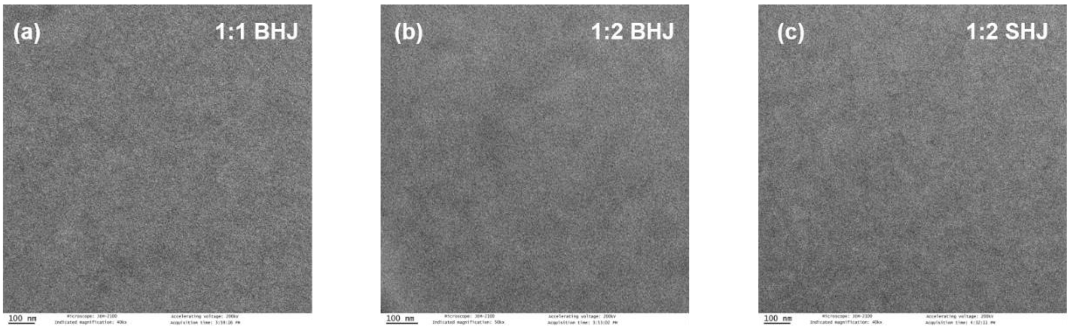

Fig. S4 TEM images of (a) 1:1 BHJ; (b) 1:2 BHJ and (c) 1:2 SHJ blend films.

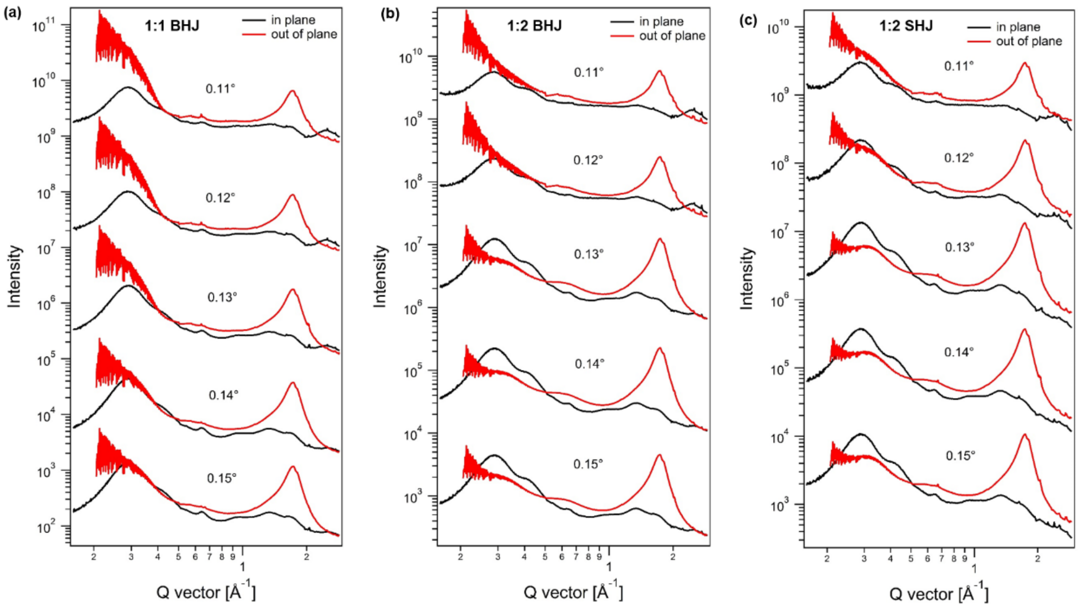

Fig. S5 GIWAXS line profiles of (a) 1:1 BHJ, (b) 1:2 BHJ and (c) 1:2 SHJ blend films with different incident angles.

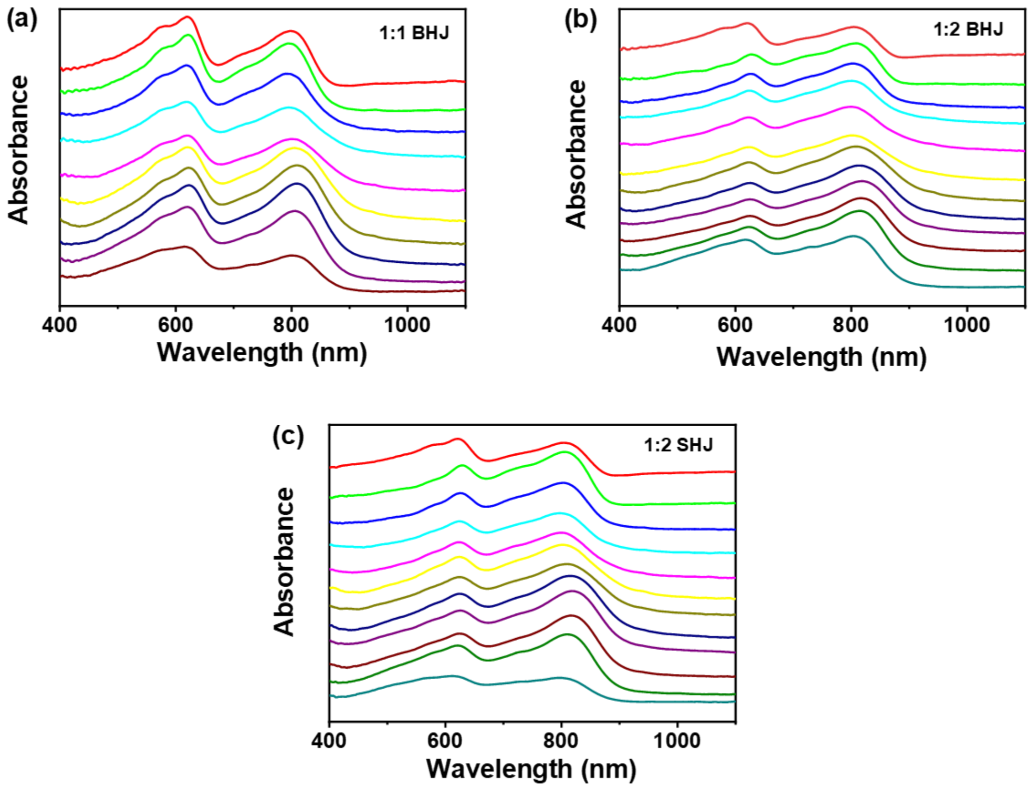

Fig. S6 Light absorption spectra of (a) 1:1 BHJ; (b) 1:2 BHJ and (c) 1:2 SHJ blend films at different film depths. For clarify, the spectra are vertically shifted. Each spectrum corresponds to a sub-film with a thickness of *ca.* 5-10 nm.

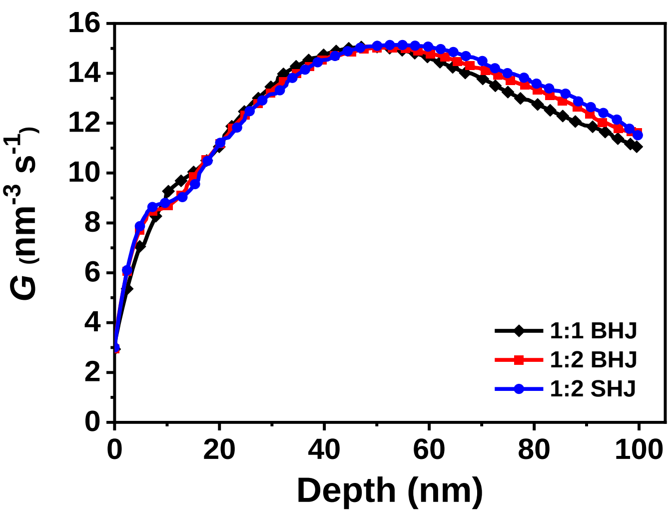

Fig. S7 Exciton generation rate *vs*. device depth profile.

Table S1 Performance of the 1:1 BHJ, 1:2 BHJ and 1:2 SHJ ST-OSCs.[a]

Active layer	Ag electrode thickness (nm)	AVT (%)	V_{OC} (V)[a]	J_{SC} (mA cm^{-2})[a]	FF (%)[a]	PCE (%)[a]	calc. J_{SC} (mA cm^{-2})
1:1 BHJ	10	21.5	0.851 (0.852±0.003)	20.6 (20.1±0.5)	66.2 (65.4±0.9)	11.6 (11.2±0.3)	20.1
	14	16.5	0.854 (0.853±0.005)	22.0 (21.4±0.4)	67.0 (65.7±1.1)	12.6 (12.0±0.4)	21.0
	17	11.7	0.864 (0.864±0.001)	22.1 (22.3±0.3)	67.3 (66.0±1.1)	12.9 (12.7±0.2)	22.4
1:2 BHJ	10	22.9	0.831 (0.831±0.003)	21.1 (20.9±0.2)	67.5 (67.0±0.5)	11.8 (11.6±0.1)	20.6
	14	16.6	0.836 (0.834±0.005)	22.6 (22.3±0.5)	67.1 (67.5±0.4)	12.6 (12.5±0.3)	21.5
	17	12.2	0.841 (0.834±0.011)	22.1 (22.1±0.5)	67.6 (67.6±0.3)	12.6 (12.5±0.2)	22.5
1:2 SHJ	10	25.4	0.831 (0.831±0.006)	21.4 (20.8±0.6)	70.6 (69.0±1.1)	12.5 (11.9±0.4)	20.5
	14	18.0	0.834 (0.835±0.002)	22.7 (22.2±0.4)	70.4 (69.7±1.1)	13.3 (12.9±0.3)	22.4
	17	12.6	0.843 (0.839±0.002)	24.0 (23.7±0.5)	69.3 (68.9±0.8)	14.0 (13.7±0.2)	23.3

[a] Average values (in parenthesis) are obtained from 15 devices

Table S2 Performance of the optimized 1:1 BHJ, 1:2 BHJ and 1:2 SHJ ST-OSCs.

device	PCE (%)	AVT (%)	APT (%)	LUE (%)	CIE coordinate	CCT (K)
1:1 BHJ	11.6	21.5	17.6	2.04	(0.2448, 0.2594)	19439
1:2 BHJ	11.8	22.9	20.2	2.38	(0.2471, 0.2669)	17133
1:2 SHJ	12.5	25.4	22.9	2.86	(0.2534, 0.2733)	14905

Table S3 Hole and electron mobilities of blend films.

active layer	μ_h ($cm^2 V^{-1} s^{-1}$)	μ_e ($cm^2 V^{-1} s^{-1}$)	μ_h/μ_e
1:1 BHJ	6.4×10^{-4}	5.4×10^{-5}	11.9
1:2 BHJ	5.6×10^{-4}	4.4×10^{-4}	1.3
1:2 SHJ	6.3×10^{-4}	7.9×10^{-4}	0.8

References

S1. A. Hexemer, W. Bras, J. Glossinger, E. Schaible, E. Gann, R. Kirian, A. MacDowell, M. Church, B. Rude and H. Padmore, *J. Phys.: Conf. Ser.*, 2010, **247**, 012007.

S2. G. G. Malliaras, J. R. Salem, P. J. Brock and C. Scott, *Phys. Rev. B*, 1998, **58**, 13411-13414.